Proceedings World Geothermal Congress 2015
Melbourne, Australia, 19-25 April 2015

Investigation of a Novel Drilling Technology – Influence of the Surface Temperature for Hydrothermal Spallation Drilling

Michael Alexander Kant, Dustin Becker, Dragana Brkic, Thierry Meier, Martin Schuler, Philipp Rudolf von Rohr

ETH Zurich, Institute of Process Engineering, Transport Processes and Reactions Laboratory, Sonneggstr.3, Zurich, Switzerland

kant@ipe.mavt.ethz.ch

Keywords: Geothermal Energy, Drilling Technology, Hydrothermal Spallation Drilling, Temperature Measurements

ABSTRACT

The drilling process accounts for about 60% of the total investment for a deep geothermal power plant. Hydrothermal Spallation Drilling (HSD) is a novel contact-free drilling technology with the potential to significantly reduce the drilling costs and therewith enhance the development of geothermal energy production. Spallation drilling is based on the effect of hard, polycrystalline rock disintegrating into small disc-like fragments, when rapidly heated by a hot fluid jet. In order to enable the spallation technology in bore holes for deep geothermal applications, a flame must be established in an aqueous environment determined by high pressures and high temperatures. Under these conditions, the critical point of water will be exceeded at a certain depth in the bore hole. In this supercritical environment light gases such as methane and oxygen form a homogenous phase with water. This mixture can be ignited, creating a so-called hydrothermal flame.

In view of increasing the efficiency of Hydrothermal Spallation Drilling, a profound knowledge of the optimal combination of the flame operating conditions and the rock properties is of utmost importance. Additionally, the spallation process itself must be thoroughly understood to enable the usage of this technology in geothermal drilling processes. Therefore, high-speed surface temperature measurements during the spallation process are reported. Rock probes are heated by two different burners while the local surface temperature during spallation is measured using two pyrometers with a maximal sampling rate of 1000 Hz and a measuring point of 1.5mm in diameter. With this setup the disintegration of single spalls is monitored as well as the induced temperature difference between surface and failure plane during the spallation process. The measured surface temperatures show a significant deviation from existing models and thus contribute to the fundamental understanding of the spallation process.

1. INTRODUCTION: BACKGROUND AND MOTIVATION

Hydrothermal Spallation Drilling is a promising novel drilling technology, with the potential to significantly reduce the drilling costs for geothermal well bores, which accounts for about 60% of the total investment costs for a deep geothermal power plant (Tester et. al. 2006). Actual conventional drilling processes for geothermal purposes or in the oil and gas industry rely on the mechanical abrasion of the rock with drilling bits. Thereby, major problems occur in drilling hard, polycrystalline rocks, leading to low rates of penetration and high wear rates of the bits. Therewith, long tripping times are required to replace the worn out bits. Hydrothermal Spallation Drilling is a contactless novel drilling technology, where a supercritical fluid jet impinges on the rock surface, inducing high local thermal stresses in the rock's upper layer, leading to the local disintegration of single rock fragments, called spalls (Wilkinson and Tester 1993) (see Figure 1). These spalls have the size of cuttings from conventional drilling processes and so can be transported away by standard drilling fluids. As drill heads for Hydrothermal Spallation Drilling are not in contact with the rock, the wear rate could be significantly reduced along with the tripping and maintenance time. This should lead to a promising reduction of the overall drilling costs ((Schuler, et al. 2012), (Augustine 2009)).

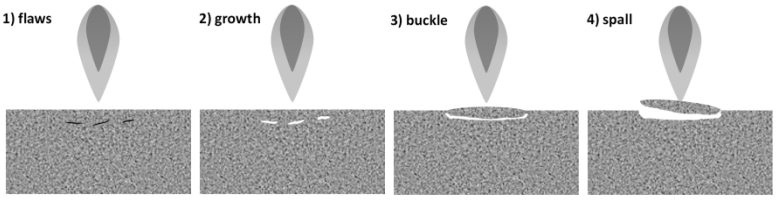

Figure 1: Illustration of the spall formation on the rock surface, due to rapid heating (adapted from (Preston 1934))

Spallation Drilling was already investigated at ambient conditions for drilling applications or quarry mining. Drilling operation with a maximal depth of 331m and penetration rates of up to 30m/h were reported (Browning, et al. 1965). The reported rates of penetration are significantly higher than commonly obtained in conventional rotary drilling of hard, polycrystalline rocks (Wilkinson and Tester 1993). Different models based on theoretical-empirical approaches were developed to describe the effect of spallation and the necessary boundary conditions for the fluid and on the rock-side. Thereby, the model developed by Rauenzahn (Rauenzahn 1986) has to be particularly highlighted. Nevertheless, the spallation effect itself is until now not thoroughly understood and a complete validation of the developed models remains undone (Wilkinson and Tester 1993). The described investigations have all been conducted at ambient conditions. For Hydrothermal Spallation Drilling no model exists and no drilling was reported yet.

Up to now, two main parameters for the description of the necessary fluid conditions for spallation drilling are reported: the heat transfer coefficient h between impinging fluid jet and the rock surface and the thereby induced surface temperature T_S of the rock.

Due to the induced thermal gradient, thermal stresses are created, leading to the local disintegration of the rock (see Figure 1). Assuming a one-dimensional heat flux in the upper layer of the rock, an energy balance around the formed spall (see Figure 2) can be formulated:

$$\frac{\lambda}{\Delta s}(\vartheta_s - \vartheta_{FP}) = h\,(\vartheta_f - \vartheta_s) \tag{1}$$

Thereby, Δs is the thickness of the released spall, ϑ_{FP} the temperature in the failure plane of the spall, ϑ_s the surface temperature, h the heat transfer coefficient and ϑ_f the temperature of the impinging fluid jet.

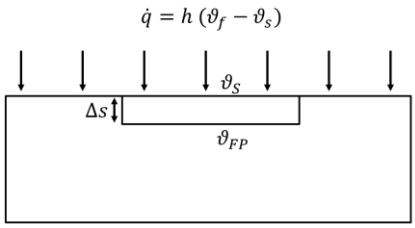

Figure 2: Boundary conditions for the formation of a single spall on the rock surface

Equation (1) shows that the heat transfer coefficient supplied by the impinging flame jet and the induced surface temperature of the rock play a major role in spallation drilling. In order to determine the necessary boundary conditions for spallation drilling at ambient or hydrothermal conditions, an accurate knowledge about these two parameters for different rock types is necessary. Additionally, in order to understand the spallation process itself, the temperature in the failure plane of the spall ϑ_{FP} must be determined. Therewith, the occurring stresses in the failure plane, leading to the disintegration of the spall, can be estimated. According to equation (1), the required fluid-side conditions for spallation drilling can be described by the heat transfer coefficient and the surface temperature. Concluding, preliminary investigations of necessary operating conditions for Hydrothermal Spallation Drilling can be conducted at ambient conditions ($p = 1bar,\ \vartheta = 20°C$) using air as surrounding fluid and transferred to hydrothermal drilling ($p > 221bar,\ \vartheta > 374°C$) in an aqueous environment. In order to determine these boundary conditions, three different rock types are investigated in this report in ambient spallation experiments: Gotthard Granite (Switzerland), Bethel Granite (USA) and Paradiso Migmatite (India). During the conducted measurements, the surface temperature ϑ_S and the failure plane temperature ϑ_{FP} are measured with two high-speed infrared pyrometers.

In several publications necessary surface temperatures for spallation drilling are reported ((Wilkinson and Tester 1993), (Rauenzahn 1986)). Wilkinson and Tester used an infrared camera with a sampling rate of 20Hz and a spatial resolution of 240 x 520 pixels. The emissivity of the rock probes was estimated with $\varepsilon = 0.90$ (Wilkinson and Tester 1993). Rauenzahn approximated the surface temperature, using equation (2):

$$\vartheta_s = \vartheta_{ro} + \frac{Q}{\lambda_r}\left(\frac{\alpha_r\, t}{\pi}\right)^{1/2} \tag{2}$$

Where ϑ_s is the approximated surface temperature, ϑ_{ro} the initial rock temperature, Q the applied heat flux, λ_r the rock thermal conductivity, α_r the rock thermal diffusivity and t the time until the first spall appears on the surface (Rauenzahn 1986). The measurements performed by Wilkinson were not able to resolve the detachment of single spalls. Rauenzahn was able to resolve this with a high-speed video camera, but had to approximate the temperature using equation (2). Concluding, the so far reported temperatures can be understood as averaged temperatures, which do not distinguish between surface temperature ϑ_S and failure plane temperature ϑ_{FP}. However, for a profound understanding of the spallation process in the rock a closer differentiation of these two temperatures is required. A detailed analysis of the literature data and a comparison with the results of this report can be found in chapter 0.

2. EXPERIMENTAL SETUP FOR AMBIENT DRILLING EXPERIMENTS

The experimental setup consists of two different burners working at ambient conditions: a 2kW butane-propane burner (Rothenberger), which collects the air for the combustion from the surroundings and requires a methane flow of $\dot{V}_{RB} \approx 0.06\,m^3n/h$, and a 7kw methane burner (Pharos), which is supplied with air by a pressurized air inlet ($\dot{V}_{Ph,air} = 2.7\,m^3n/h$) and uses a methane flow of $\dot{V}_{Ph,CH4} = 0.3\,m^3n/h$. Both burners applied for the experiments can be controlled by flow controllers and create flame temperatures of about $\vartheta_f = 1250\,°C$.

The flames of the described burners impinge vertically onto the 250mm x 250mm x 150mm large rock probes. Thereby, the stand-off distance (SOD) between the outlet nozzle of the burners and the surface of the rock is adjusted to SOD=50mm. During the drilling process the SOD is not changed from the preliminary adjustment. Due to the induced thermal stresses in the rock probes, the spallation process starts after approx. 20 sec. and cavities with a diameter of 40 mm to 50 mm and a depth of approx. 30mm are formed.

The surface temperature during the spallation process is measured with two OPTRIS OPTCTL3MH2CF2 pyrometers. These pyrometers can measure temperatures from 200°C up to 1500°C with a sampling rate of 1000Hz at a wavelength of $\lambda = 2.3\mu m$. As the pyrometers only receive 90% of the signal in 1ms with a sampling rate of 1000Hz, all data reported are measured with a sampling rate of 500Hz. The focus spot of the pyrometers has a diameter of 1.5mm. With this small measuring spot it is possible to

resolve the detachment of single spalls, which are in the size of 2mm-10mm. Additionally, a video camera is installed, allowing a later visual observation of the experiments.

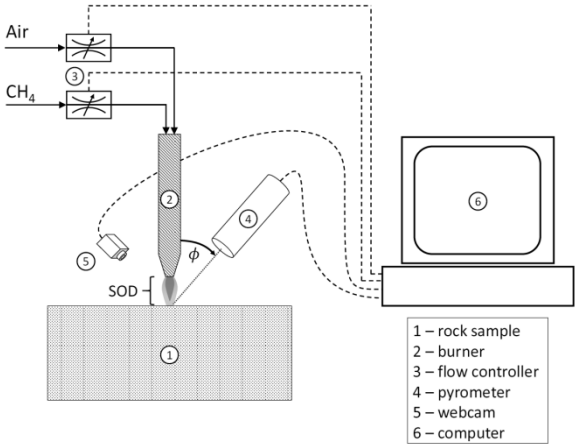

Figure 3: Experimental setup for surface temperature measurements during the spallation process

3. INFRARED SURFACE TEMPERATURE MEASUREMENTS

3.1 Emissivity Measurements

The emissivity of the investigated rock probes is a crucial point for determining the surface temperature during the spallation process. As the emissivity depends highly on the emitted wavelength, generally for an accurate measurement no literature data can be used and the emissivity has to be measured for every single pyrometer type. Additionally, as the emissivity varies with the applied measuring angle ϕ (see Figure 3), the angle is kept constant for all described measurements in this report with $\phi \approx 30°$.

Different ways to determine emissivities in a required wavelength range are possible. For the presented experiments the determination based on a reference emissivity is applied. Therefore, the color PYROMARK 2500, a silicon-based high-temperature paint for solar thermal purposes with a high temperature resistance and excellent optical properties (high absorbance and high emissivity), is used. The color was chosen, as reliable data for the emissivity of this color and other properties exist, e.g. the required pretreatment of the color (Roderick Mahoney, et al. 2012). In order to confirm the data from literature, the emissivity of the color was measured and compared with the above quoted data. The results of this experiment show the same values as stated in literature.

Based on the emissivity values of PYROMARK 2500, the emissivity of the different investigated rock types can be derived. Therefore, the rock is partially painted with the color and heated up. After the heating process, the rock is placed under two identical pyrometers. Pyrometer 1 measures the temperature on the colored area (see Figure 4). As the emissivity is known, Pyrometer 1 indicates the correct temperature. Pyrometer 2 measures on the not colored rock surface, directly next to the colored area. The emissivity of the rock is now derived by adjusting the emissivity input value of Pyrometer 2 until the temperature fits with the temperature displayed by Pyrometer 1.

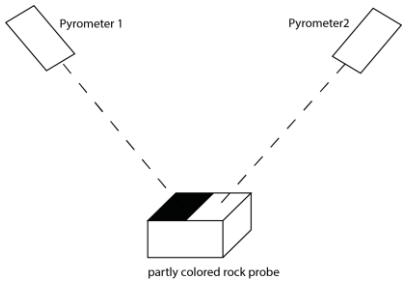

Figure 4: Setup for determining the emissivity of rock probes at different surface temperatures

Figure 5 shows the emissivity results of the investigated rock types for different temperatures. Additionally, an average value is stated, including an upper and lower uncertainty range. Due to the heterogeneous composition of the rock, the emissivity values vary considerably among the different measurements. As the emissivity stays almost constant over the investigated temperature range, averaged emissivity values can be used for the surface temperature measurement.

It has to be considered that the reported values only account for the operating wavelength range ($\lambda = 2.3\mu m$) and the applied angle ($\phi \approx 30°$) of the installed pyrometers. Therewith, it is not unusual that the emissivity values differ from values stated in literature. As the adjustment of the emissivity in the pyrometers takes about one second, it is not possible to adjust the emissivity during the spallation process. Therefore, average emissivity values are chosen for the surface temperature measurements during the spallation process. The thereby occurring error is taken into consideration in the total error estimation.

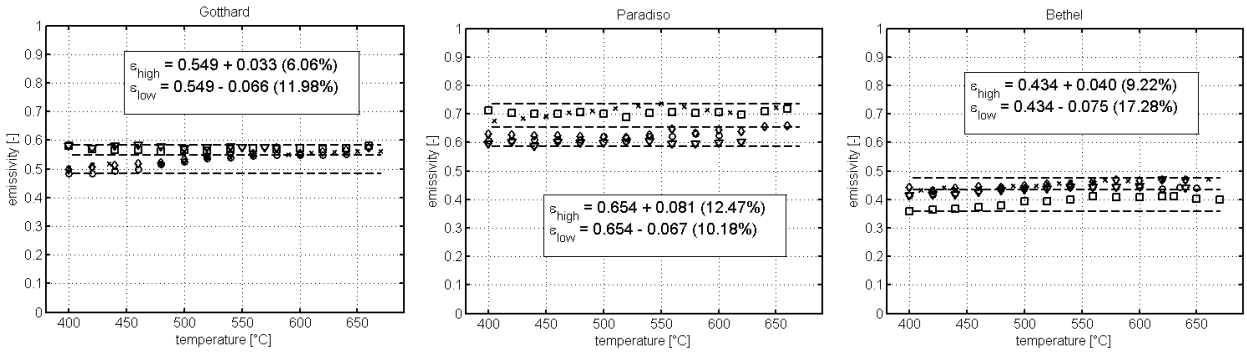

(a) (b) (c)

Figure 5: Spectral directional emissivity at different surface temperatures of: (a)Gotthard Granite, (b) Paradiso Migmatite, (c) Bethel Granite

3.2 Error Estimation

As spallation drilling is a high-speed transient effect, a precise and reliable measurement procedure is necessary to determine the surface temperature during the drilling process as accurately as possible. Therefore, an extensive error estimation is conducted. As the surface temperature measurement relies on the emissivity of the measured surface, the influence of the uncertainty of the emissivity on the surface temperature measurement is investigated. Additionally, the error induced by the impinging flame is identified.

3.2.1 Error due to the Uncertainty of the Emissivity of the Investigated Rock Types

In order to precise the surface temperature measurement, the influence of the uncertainty of the emissivity on the surface temperature measurement is determined. Therefore, the pyrometer is focused on an electrical heater coated with a color of known emissivity. The influence of the emissivity is obtained by changing the emissivity of the pyrometer to a lower value than the correct one and monitoring the received temperature difference of the pyrometer. The relative temperature difference $\Delta\vartheta$, due to the emissivity change $\Delta\varepsilon$ can be calculated by equation (3).

$$\Delta\vartheta = \frac{\vartheta_{\varepsilon} - \vartheta_{\Delta\epsilon}}{\vartheta_{\varepsilon}} \tag{3}$$

Where ϑ_{ε} is the temperature measured with the right emissivity and $\vartheta_{\Delta\epsilon}$ is the temperature measured with the adjusted emissivity. The procedure described above is repeated for different reference surface temperatures of the electrical heater. The collected data is summarized in Figure 6.

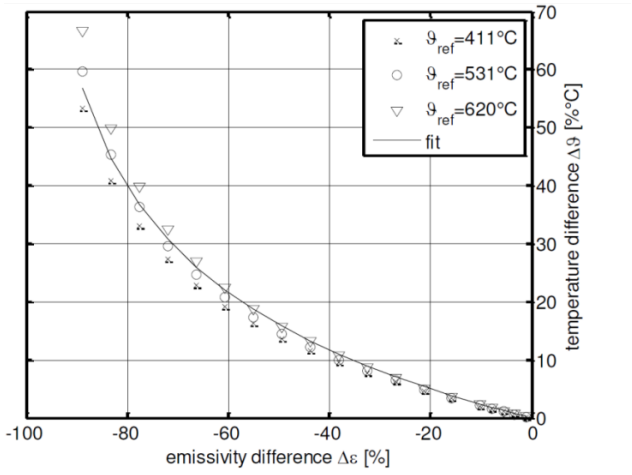

Figure 6: Sensitivity of the emissivity uncertainty on the temperature measurement

Figure 6 shows that high uncertainties in the emissivity measurement have a low impact on the pyrometer. For example, an emissivity error of $\Delta\varepsilon = 20\%$ implies a temperature difference of only $\Delta\vartheta = 5\%$. Therewith, the uncertainty of the emissivity measurement is not a determining factor. Additionally, it can be observed that the surface temperature does not play a role for moderate emissivity differences.

The relative error in the surface temperature due to the uncertainty in the emissivity measurement can be stated, according to the intern conversion of the temperature in the infrared sensor, as:

$$d\vartheta_\varepsilon = \frac{1}{\vartheta_{obj} - 273.15}\left[\left(\frac{\vartheta_{obj}^n + d\varepsilon \cdot \vartheta_{amb}^n}{1 + d\varepsilon}\right)^{1/n} - \vartheta_{obj}\right] \quad (4)$$

As the exponent n is unknown, the theoretical curve described by equation (4) can be fitted to the experimental data shown in Figure 6. Thereby, the exponent n is sensitive to the object temperature and the fitted data. A very precise fitting, as shown in Figure 6, was achieved with a fixed object temperature of $\vartheta_{obj} = 823.15K$, an ambient temperature of $\vartheta_{amb} = 293.15K$ and $n = 6.8$.

3.2.2 Influence of the Flame on the Surface Temperature Measurement

In order to guarantee a precise measurement of the surface temperature, the influence of the flame on the measurement is investigated with an experimental setup: two pyrometers measure the same spot of an adjustable electrical heater. One of the pyrometers is disturbed by the flame, as the other pyrometer measures the undisturbed temperature. With the collected data it is possible to quantitatively determine the difference between the disturbed and undisturbed measurement for different surface temperatures and therewith derive the influence of the flame on the surface temperature measurement. High fluctuations in the measurement induced by the flame can be monitored and are indicated by the error bars in Figure 7. Additionally, the flame generates an offset of the average value to the measurement of the undisturbed pyrometer.

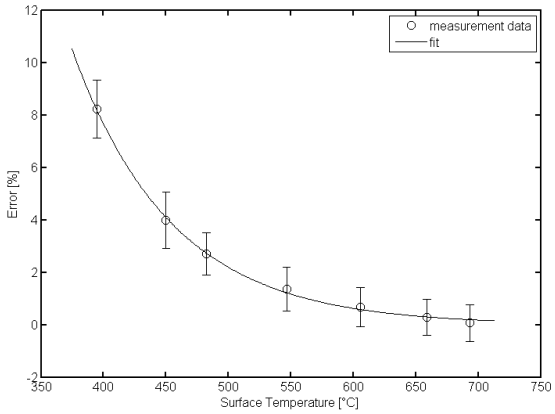

Figure 7: Influence of the flame on the surface temperature measurement

The error in the surface temperature measurement due to the disturbance by the flame is approximated by equation (5):

$$d\vartheta_{flame} = 11.6 \cdot \exp(-0.01255 \cdot \frac{\vartheta}{°C}) \quad (5)$$

The evaluated data shows that the influence of the flame is strong at low temperature ranges. However, in the temperature range were spallation is expected ($\vartheta = 500 - 700°C$) the influence of the flame on the averaged surface temperature plays a minor role. As the fluctuations caused by the turbulences of the exhaust gases are still disturbing the measurement, the temperature before and after the detection of a spall has to be averaged (see chapter 0).

3.2.3 Overall Error for the Surface Temperature Measurement

The total error of the surface temperature measurement can be calculated according to:

$$d\vartheta_{ges}^2 = \sum d\vartheta_i^2 = d\vartheta_{sys}^2 + d\vartheta_{Flame}^2 + d\vartheta_\varepsilon^2 \quad (6)$$

Thereby, $d\vartheta_{Flame}$ is the error due to the influence of the flame on the measurement, $d\vartheta_\varepsilon$ is the error due to the uncertainty in the emissivity measurement and $d\vartheta_{sys}$ is the systematic error of the pyrometers definded by the manufacturer and calculated by equation (7).

$$d\vartheta_{sys} = \frac{0.003 \cdot \vartheta + 2°C}{\vartheta} \quad (7)$$

Figure 8 shows the total error as a function of the measured surface temperature. As the relative error accounts for only 5% to 6%, in the temperature range interesting for spallation drilling, accurate surface temperature measurements are possible with the described measuring principle. Additionally, the absolute error function of the measurement presents a minimum at a surface temperature of approx. $T_s = 500°C$, which is near the main temperature were spallation will be detected, as will be shown in the following chapters of this report.

In the total error calculation, the highest deviation from the emissivity measurement of all rock types ($d\varepsilon_{Bethel} = 17\%$) was chosen. In order to simplify the calculation, the temperature dependency of the influence of the emissivity uncertainty was neglected and a reference temperature of $T_{obj} = 600°C$ (see chapter 0) was used for this investigation.

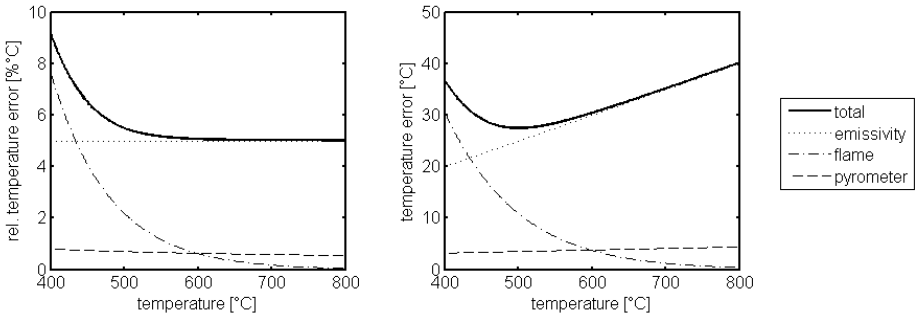

(a) (b)

Figure 8: (a) Relative and (b) absolute error of the surface temperature measurement

4.RESULTS AND DISCUSSION

In the following chapter the results of the surface temperature measurement are reported. Three different measurements are conducted for every rock probe and every operating condition. As described above, the measurements were conducted with two different burners (Pharos and Rothenberger) at a stand-off distance of 50mm.

4.1 Processing of the raw data

Figure 9 shows a typical surface temperature over time plot of the experimental raw data. It can be observed that the temperature rises within a few seconds to about 600°C and spallation starts, indicated by a rapid temperature drop and followed by a next heating period until the next spall detaches. Additionally, the mean temperature rises over time, caused by overheating of the rock. This means that less heat is rejected with the spalls than delivered by the flame impinging on the rock. As a next step in the post-processing all detected spalls have to be investigated separately.

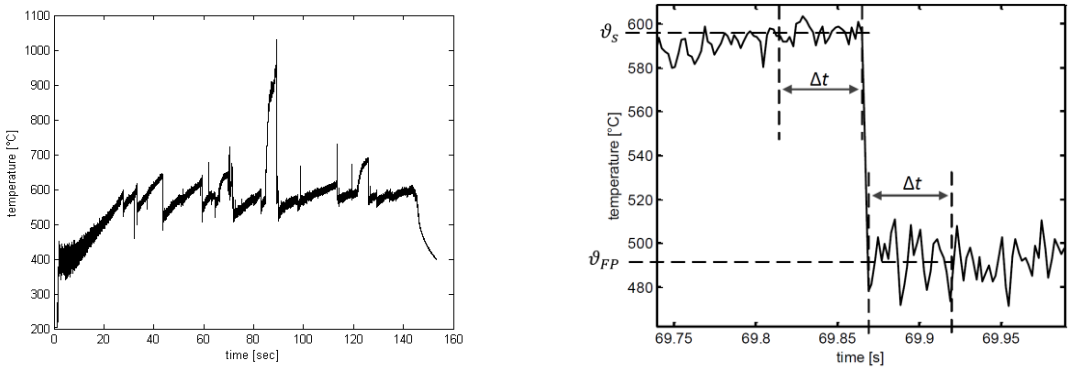

(a) (b)

Figure 9: (a) Typical figure of the acquired raw data of the surface measurement, (b) detachment of a single spall

First the recorded video is analyzed to guarantee that a spall has detached from the area where the pyrometer is focused (indicated by lasers) and that the observed temperature drop is not caused by a distortion of the pyrometer. Additionally, it must be confirmed that the detected spall is larger than the diameter of the measuring spot to ensure a precise measurement. Otherwise, the measured temperature in the failure plane of the spall ϑ_{FP} after the detachment of the spall will be an average of the recently created surface and the surrounding area. Figure 9 shows that the spallation process induces a temperature difference of approx. $\Delta\vartheta = 100°C$ in a few milliseconds. In order to exactly determine this temperature difference, the temperature before and after the detachment of a spall is averaged over a time period of $\Delta t = 5ms$. Therewith, the influence of the fluctuations of the flame is minimized (see chapter 0). Due to the short time period, the influence of a further heating of the rocks surface can be neglected.

4.2 Surface Temperatures of the Investigated Rock Types

As stated above, three different rocks are investigated in this report: Gotthard Granite (Switzerland), Bethel Granite (USA) and Paradiso Migmatite (India). For every experiment the post-processing as described above is applied. Figure 10 shows two exemplary plots for the surface temperatures and the temperatures in the failure plane for spallation experiments conducted on Gotthard Granite.

Regarding Figure 10 (a), it can be seen that the surface temperature ϑ_S varies among the different detected spalls, whereas the temperature in the failure plane of the spall ϑ_{FP} stays nearly constant. As ϑ_{FP} directly indicates the thermal stresses in the rock, leading to the failure and therewith the detachment of the spalls, it can be concluded that the occurring stresses stay nearly constant for every spall. So a closer investigation of this thermal stresses in the failure plane is necessary for a deeper understanding of the spallation effect. Additionally, considering constant stresses leading to the formation of the spalls, the variation of the surface temperature ϑ_S can be explained by the varying thickness of the rejected spalls. Comparing Figure 10 (a) and Figure 10 (b), it can

be seen that the temperature difference $\Delta\vartheta = \vartheta_S - \vartheta_{FP}$ is smaller for the experiment conducted with the Pharos burner than for the experiment conducted with the Rothenberger burner. Due to the higher heat transfer coefficient of the Pharos burner, thinner spalls are created and therewith, according to equation (1) a smaller temperature difference is detected. Additionally, it can be observed, that for Figure 10 (a) the temperature in the failure plane of the spall ϑ_{FP} stays relatively constant. This means that nearly all the heat induced by the flame is rejected by the detaching spalls. In Figure 10 (b) the temperature rises over the time, indicating that the rock is overheating in the second presented experiments, due to non-optimal operation conditions. Nevertheless, the temperature rise might level off if the experiment is conducted longer, leading to stable operation conditions. Figure 11 summarizes all data of the reported experiments.

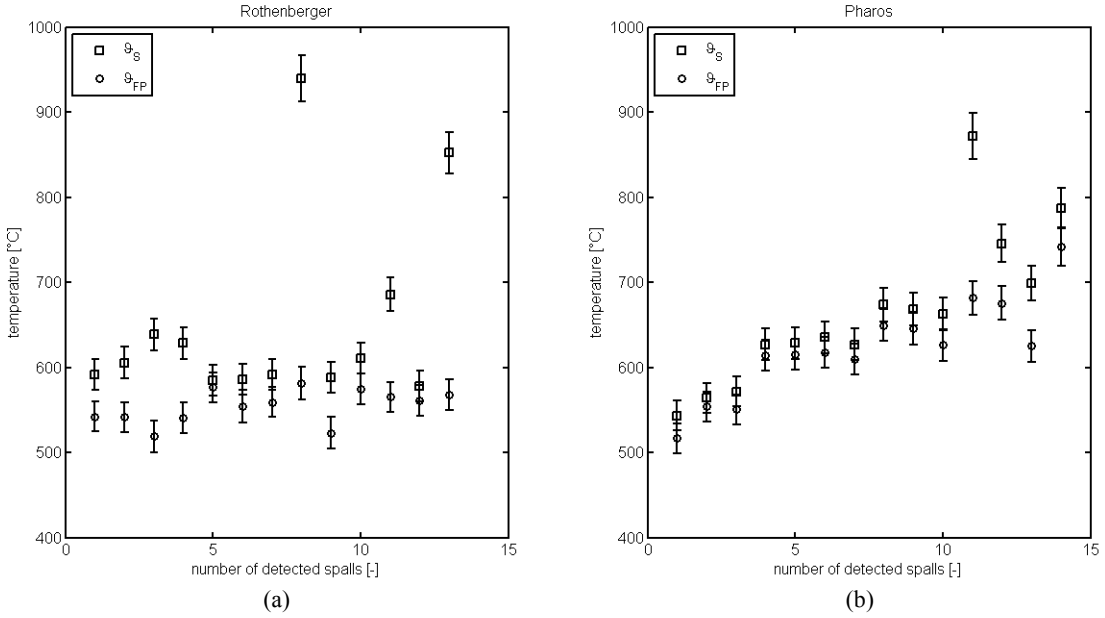

Figure 10: Results of the surface temperatures and the temperatures in the failure plane for Gotthard Granite; pallation experiments are conducted with the (a) Rothenberg burner and (b) Pharos burner

	Heat Flux	Temperatures			No. spalls investigated
	$\dot{q}$ [MW/m^2]	ϑ_S [°C]	ϑ_{FL} [°C]	$\Delta\vartheta$ [K]	# [-]
Gotthard					
Rothenberger	0.64 ± 0.10	633 ± 71	573 ± 45	≈ 60	59
Pharos	0.83 ± 0.13	659 ± 81	605 ± 60	≈ 54	70
Bethel					
Rothenberger	0.66 ± 0.09	610 ± 52	552 ± 44	≈ 62	53
Pharos	0.88 ± 0.09	629 ± 55	578 ± 53	≈ 51	29
Paradiso					
Rothenberger	0.69 ± 0.11	580 ± 67	519 ± 49	≈ 61	62
Pharos	-	-	-	-	-

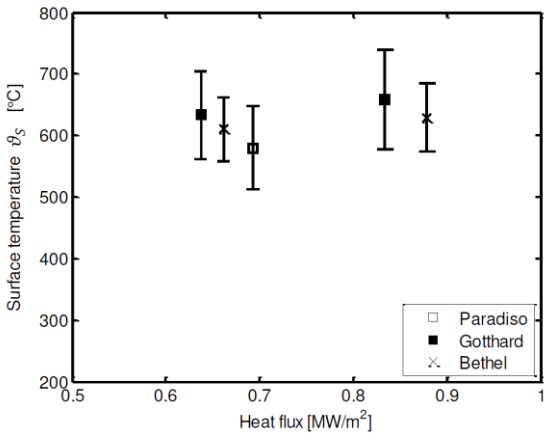

Figure 11: Summary of the reported surface temperature measurements with the according heat fluxes

Regarding Figure 11, the temperature range indication is not the error on the measurement, but the deviation in-between all detected spalls. This is significantly higher than the measuring error which accounts for only 5-6% of the surface temperature as described in chapter 0. The high fluctuation in the temperatures originates from the heterogeneous composition of the rock. The heat fluxes stated in Figure 11 are approximated with a heat flux sensor, consisting of a copper rod placed inside a cylindrical stainless steel housing. The temperature distribution inside the copper rod is measured at two positions with thermocouples. The heat flux measured by this sensor is then transferred to the heat flux of the rock, by assuming a constant heat transfer coefficient h on the sensor and on the rock surface.

4.3 Comparison with Available Data

In order to confirm the reliability of the proposed principle for surface temperatures measurements during the ambient spallation process, the reported data is compared in Figure 12 with data available in literature ((Wilkinson and Tester 1993), (Rauenzahn 1986)).

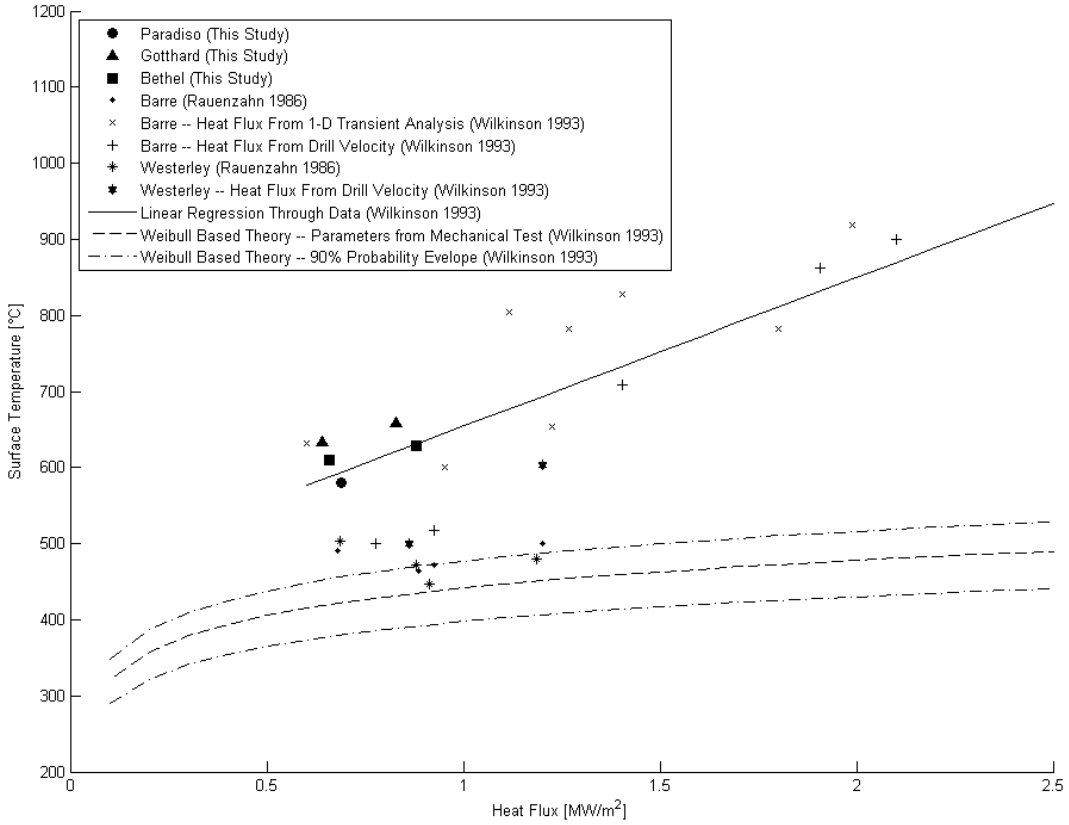

Figure 12: Comparison of the measured surface temperatures and the heat fluxes with reported data by Wilkinson and Rauenzahn; Weibull Data from Barre Granite, assuming physical properties at 573K; adapted from (Wilkinson and Tester 1993)

The results from this study are well within the range reported by Wilkinson. Both data show that the surface temperature increases linear with the heat flux, as it can be calculated by assuming a one-dimensional heat flux through the upper layer of the rock. According to the data of this report and the data of Wilkinson, it seems like that the Weibull Based Theory, developed by Rauenzahn does not predict the surface temperatures and heat fluxes occurring in spallation drilling accurately enough, if the required Weibull parameters are obtained from mechanical tests at ambient conditions. Therefore, it can be concluded that an application of this model for spallation drilling might not be possible and the development of a new model in accordance with the reported measurements should be pursued. Nevertheless, the validation of Wilkinson's data for higher heat fluxes remains so far open and will be done in the future. Additionally, it has to be highlighted that a fitting of the Weibull Based Theory to the received data is possible (see (Wilkinson and Tester 1993)) and shows good accordance with the experimental data. Furthermore, according to the data described in this report and by Wilkinson, it can be concluded that the α-β quartz phase transition in granite, appearing at about 573°C, and implying a significant increase of the thermal expansion (Bauer und Handin 1983), could contribute to the spallation process. Nevertheless, the role it plays remains unknown and has to be investigated in further research.

4.4 Comparison Ambient Spallation Drilling – Hydrothermal Spallation Drilling

According to equation (1), the spallation effect only depends on the heat transfer coefficient gained through the impingement of the fluid on the rock and on the induced surface temperature. Concluding, preliminary investigations of necessary operation conditions for Hydrothermal Spallation Drilling can be conducted at ambient conditions ($p = 1bar, \vartheta = 20°C$) using air as surrounding fluid and transferred to hydrothermal conditions ($p > 221bar, \vartheta > 374°C$) in an aqueous environment. Nevertheless, in these aqueous, high-pressure conditions the inclusion of water into the rock can have an influence, which is at the moment still unknown. Additionally, the physical properties of the rock vary with temperature and pressure. At great depths, as they occur in drilling for geothermal and oil-and-gas purposes, the maximal compressive strength of the stone is significantly lower (Mogi 1965), which could have an important effect on the spallability of the rock formation. Especially, the transition from brittle fracture to ductile flow is of particular interested for the spallation process. The influence of these different parameters on Hydrothermal Spallation Drilling will be reported in the future. With a novel high pressure pilot plant located at ETH Zurich, first preliminary Hydrothermal Spallation Drilling experiments were conducted (Stathopoulos 2013). The results have shown that heat transfer coefficients of $h = 1500\ W/(m^2\ K)$ and flame temperatures of $\vartheta_f = 1200°C$ could be reached. As these conditions are similar to the operation conditions reported in this study, Hydrothermal Spallation Drilling should be possible according to Figure 12.

5. CONLUSIONS

In the present study a precise and reliable procedure for local high-speed surface temperature measurements during the ambient spallation process were reported. This procedure is able to resolve the detachment of single spalls during the spallation process and to determine the surface temperature ϑ_s directly before the disintegration of the spall and the temperature in the thereafter exposed failure plane of the spall ϑ_{FP}. The error in the measurement procedure accounts for 5-6% of the surface temperature in the for

spallation interesting temperature range. With the described procedure three different rock types were investigated according to the necessary operation conditions for spallation drilling. The experiments were done with two different burners at heat flux rates of $\dot{q} = 0.64 - 0.88\ MW/m^2$. Surface temperatures from $\vartheta_s = 580°C$ up to $\vartheta_s = 659°C$ were measured and the temperature in the failure layer of the rock accounts from $\vartheta_{FL} = 519°C$ up to $\vartheta_{FP} = 605°$. The results of these experiments are in good agreement with results reported by Wilkinson (Wilkinson and Tester 1993). The report supports Wilkinson's statement that the Weibull Based Theory developed by Rauenzahn seems not to predict the surface temperatures and heat fluxes occurring in spallation drilling accurately enough, if the required parameters are obtained from mechanical experiments. Therewith, the development of a novel model might be required. Especially, considering an application of the spallation effect at hydrothermal conditions for deep drilling operations the necessary operating conditions have to be known and the effects appearing during the spallation process have to be understood.

BIBLIOGRAPHY

Augustine, Chad R. Hydrothermal Spallation Drilling and Advanced Energy Conversion, Technology for Engineered Geothermal Systems. PhD Thesis, Massachusetts Institute of Technology, 2009.

Bauer, Stephen J., and John Handin. "Thermal Expansion and Cracking of Three Confined, Water-Saturated Igneous Rocks to 800°C." Rock Mechanics and Rock Engineering 16, 1983: 181-198.

Browning, J. A., W.B. Hortin, H. E. Fletcher, and H. L. Hartman. "Recent Advances in Jet Working of Minerals." Seventh Symposium on Rock Mechanics. Pensylvania State Universtiy, 1965.

Mogi, Kiyoo. "Pressure Dependence of Rock Strength and Transition from Brittle Fracture to Ductile Flow." Bulletin of the Earthquake Research Institute, Vol. 44, 1965: 215-232.

Preston, F. W. "Observations of Spalling." Journal of the American Ceramic Society, Vol. 17, 1934: 137-144.

Rauenzahn, Rick Meier. Analysis of Rock Mechanics and Gas Dynamics of Flame-Jet Thermal Spallation Drilling. PhD Thesis, Massachusetts Institute of Technology, 1986.

Roderick Mahoney, A., Andrea Amborsini, Clifford Ho, Marlene Bencomo, Aaron Hall, and Timothy Lambert. "Characterization of Pyromark 2500 for High-Temperature Solar Receivers." ASME 2012 6th International Conference on Energy Sustainability. San Diego, CA, USA, 2012.

Schuler, M., T. Rothenfluh, P. Statopoulus, D. Brkic, and P. Rudolf von Rohr. "Supercritical Water Jets Penetrating Subcritical Water - Application for Hydrothermal Spallation Drilling ." Thirty-Seventh Workshop on Geothermal Reservoir Engineering . Stanford, CA, USA, 2012.

Stathopoulos, Panagiotis. Hydrothermal Spallation Drilling - Experiments in a Novel High Pressure Pilot Plant. PhD Thesis, Zurich, Switzerland: ETH Zurich, 2013.

Tester et. al., Jefferson W. "The Future of Geothermal Energy: Impact of Enhanced Geothermal Systems (EGS) on the United States in the 21st Century." Massachusetts Institute of Technology, 2006.

Wilkinson, M. A., and J. W. Tester. "Experimental Measurement of Surface Temperatures During Flame-Jet Induced Thermal Spallation." Rock Mech. Rock Engng. (1993) 26 (1) (Rock Mech. Rock Engng.), 1993: 29-62.